NSS
Neutrosophic Sets and Systems, Vol. 98, 2026
University of New Mexico

A Neutrosophic Rayleigh Approach Based on DUS-Transformation for Analysing COVID-19 Incubation Periods

Meenakshi Gautam

Department of Mathematics, School of Advance Science,
Vellore Institute of Technology (VIT), Vellore, Tamilnadu, India.

* Correspondence: Meenakshi Gautam, meenakshi.gautam@vit.ac,in

Abstract: The DUS transformation to the Rayleigh distribution introduces better modelling of real-world variations and enhances its ability to represent skewed or heavy-tailed data. To address ambiguity, inconsistency, and indeterminacy in data, In this study, we introduce an extension of the neutrosophic Rayleigh distribution, the DUS Transformed Neutrosophic Rayleigh (DUSNR) Distribution. Important statistical aspects of the DUSNR distribution, such as quantiles, moments, moment-generating functions, and order statistics, are determined under neutrosophic conditions. The performance of the maximum likelihood estimator is assessed by simulation, showing that its accuracy increases as sample sizes rise. Lastly, the findings of applying the suggested distribution to the COVID-19 incubation dataset are contrasted with those of the DUS transformed Rayleigh distribution and the neutrosophic Rayleigh distribution.

Keywords: Neutrosophic; DUS transformation; Probability distribution; Rayleigh distribution

1. Introduction

In many real-world problems, traditional statistics assumes exact values, but in practice, uncertainty and indeterminacy often make data imprecise, vague, or ambiguous. The classical statistical methods become less effective in this case because they rely on precise numerical inputs. Recently, there have been several developments in modelling such imprecise situations by taking into account fuzzy logic and neutrosophy; refer to Atanassov (1999), Zeina and Hatip (2021) and Belohlavek et. al (2017). To address indeterminacy or partially ambiguous aspects in the data, Vladutescu and Colhon (2020) Proposed neutrosophic statistics and denoted the components as T, I, and F, which stand for truth, indeterminate, and falsehood, respectively.

Neutrosophic is a multiple-valued logic that makes a distinction between imprecise probability, fuzzy logic, and classical logic. Many branches of science and engineering have used this line of thinking. Neutosophic logic-based probability distributions have been used in several investigations. Neutosophic probability distributions, such as the normal and binomial distributions, were created by Patro and Smarandache (2016). Alhabib et al. (2018) generalised the corresponding classical distributions to introduce neutrosophic Poisson, uniform, and exponential distributions. Alhasan and Smarandache (2019) investigated the neutrosophic Weibull distribution and its related family of neutrosophic distributions. Khan et. al (2021) introduced the neutrosophic Rayleigh distribution under the neutrosophic statistics and discussed its various properties. Sherwani et al. (2021) identified numerous statistical features of the traditional beta distribution and expanded it to a neutrosophic context. The distribution was applied to two real-world datasets to validate the results.

Khan and Al-Bossly (2021) established the Gamma distribution under indeterminacy with applications to complex data analysis. For modelling Nitrogen oxide emissions data of Denmark, in 2022, Khan and colleagues came up with a neutrosophic lognormal distribution. The neutrosophic Kumaraswamy distribution was suggested by Ahsan-ul-Haq (2022) for the analysis of constrained data sets in an environment of indeterminacy.

In 2023 onwards, more distributions about imprecise data were introduced. Norouzirad et al. (2023) introduced the neutrosophic generalised Rayleigh distribution and showed that the distribution is ideal to model skewed lifetime data. Rao (2023) established a neutrosophic log-logistic distribution model in complex alloy metal melting point applications. Neutrosophic beta-Lindley distribution was established by Algamal et al. (2024) to model bladder cancer data. Neutrosophic Birnbaum-Saunders distribution for imprecise data was introduced by Hassan and Aslam (2024), and the results were validated through datasets based on alloy melting points and the lifetime of batteries. Jamal et al. (2024) proposed neutrosophic BURR-III to model COVID-19 data. Recently, Aslam (2024) established the neutrosophic negative binomial distribution and developed algorithms for generating data based on this distribution.

Due to its simplicity and lack of extra parameters, the DUS transformation produces a parsimonious distribution**.** Khan and Mustafa (2023) applied the DUS transformation to the powered inverse Rayleigh distribution and derived key statistical properties, including moments, entropy, and stress-strength reliability, along with the maximum likelihood estimator (MLE). Banerjee and Bhunia (2022) introduced the Exponential Transformed Inverse Rayleigh distribution via the DUS transformation, studying its key properties and discussing four estimation methods, including maximum likelihood, maximum product spacing, least squares, and weighted least squares methods. Tripathi and Agiwal (2024) obtained similar results for the DUS-Rayleigh distribution and further evaluated the Cramér–Von Mises estimator, using the squared error loss function for Bayesian estimation.

1.1 *Contribution of the paper*

This study proposes a novel DUS Transformed Neutrosophic Rayleigh (DUSNR) distribution. The main objective of the suggested distribution is to integrate the unknown data on the variables being examined into the current classical distribution. The suggested model shows a better fit than current Rayleigh-based models when it is finally applied to COVID-19 incubation time data.

The paper is organised as follows. The suggested model and related charts are shown in Section 2. In Section 3, the statistical features are obtained. In Section 4, a parametric estimate is made. Section 5 explains the simulation research. Section 6 includes a real data set research, and Section 7 concludes the findings.

1.2 *Importance of neutrosophic in this work*

The data are not always clear when we look at COVID-19 incubation periods. Some cases are reported exactly, like "the incubation was 7 days." In other cases, like "between 5 and 7 days," the information is not clear because the exact day of exposure is not known. There are also times when the data do not agree or have errors, like when two sources give different incubation times for the same patient. The data must be precise and consistent for classical statistical models to function effectively, which is not the case in this case. Because it can handle precise values, ambiguous ranges, and even contradicting records together, a neutrosophic model is helpful. This enables us to utilise all of the data without oversimplifying it, producing more trustworthy results for COVID-19 research conducted in the real world. Our goal is to ensure that our model accurately captures the uncertainty

inherent in COVID-19 data so that the inferences made can more confidently inform real-world decisions.

2. The DUS-transformed neutrosophic Rayleigh distribution

This section presents a new DUSNR distribution using a baseline neutrosophic Rayleigh distribution. Let the non-negative neutrosophic random variable. $\boldsymbol{X_N = X_L + X_U\, I_N}$ Follow the baseline Rayleigh distribution, where the determinacy is presented in the first part and the indeterminacy measure. $\boldsymbol{I_N}$ lying within the interval $[\boldsymbol{I_L},\ \boldsymbol{I_U}]$, reflects the indeterminacy of the neutrosophic form.

For scale parameter $\theta > 0$ and $\boldsymbol{X_N} > 0$, the probability density function (pdf) of the neutrosophic Rayleigh distribution is given as

$$\boldsymbol{f_N(x_N) = (1 + I_N)\, 2\theta x_N e^{-\theta x_N^2},\ x_N > 0} \tag{1}$$

The neutrosophic cumulative distribution function (CDF) that corresponds to this is computed as

$$\boldsymbol{F_N(x_N) = \int_0^{x_N} f_N(t)\, dt = (1 + I_N)\left(1 - e^{-\theta x_N^2}\right)} \tag{2}$$

We introduce the DUSNR distribution using the PDF in (1) and the CDF in (2). The DUS neutrosophic PDF and DUS neutrosophic CDF for the proposed distribution are given by

$$\boldsymbol{g_{DUSNR}(x_N) = \frac{f_N(x_N)}{e-1} e^{F_N(x_N)} = \frac{(1 + I_N)2\theta x_N e^{-\theta x_N^2}}{e-1} e^{(1+I_N)\left(1-e^{-\theta x_N^2}\right)},\ x_N > 0} \text{ and}$$

$$\boldsymbol{g_{DUSNR}(x_N) = \frac{e^{F_N(x_N)}-1}{e-1} = \frac{e^{(1+I_N)\left(1-e^{-\theta x_N^2}\right)}-1}{e-1},\ x_N > 0,} \tag{3}$$

respectively, with their corresponding plots presented in Figure 1.

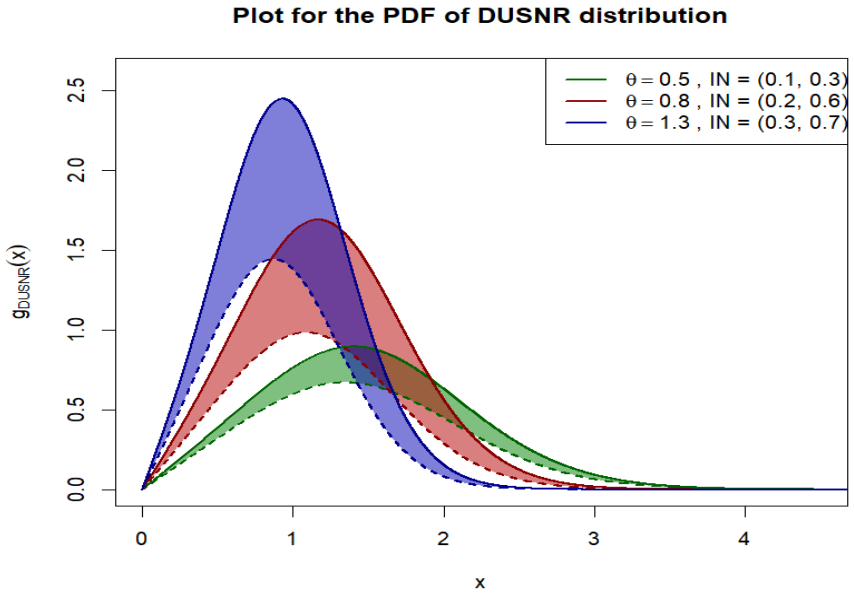

(a)

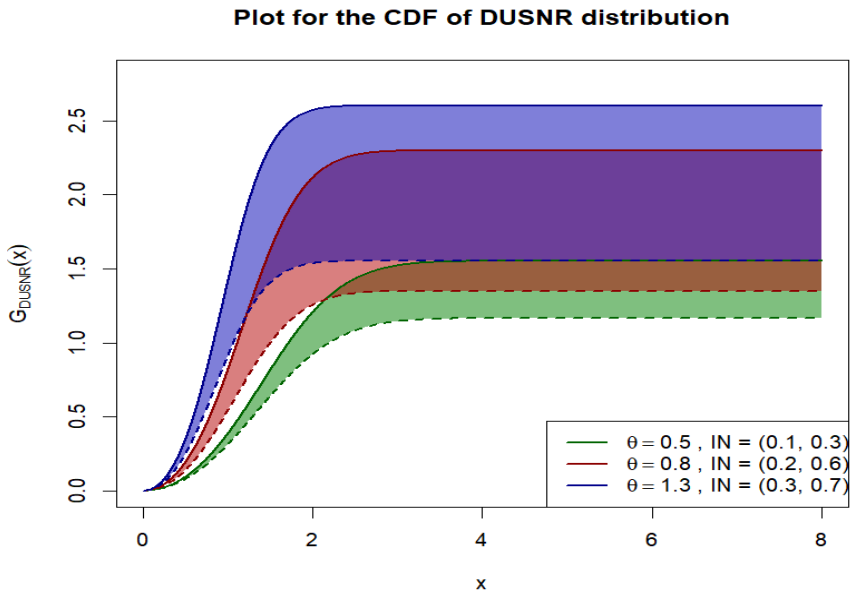

(b)

Figure 1: The plots for (a) PDF, (b) CDF of DUSNR distribution using different values of I_N

Theorem: The DUSNR distribution is unimodal if $x_N^2 > ln(1 + I_N)\,/\theta$.

Proof: By definition, the mode of the distribution is determined by solving the equation $g'_{DUS}(x_N) = 0$, Which represents the derivative of the density function with respect to x_N. Now, we prove the uniqueness of this mode. Let

$$\ln(g_{DUSNR}) = \ln x_N - \theta x_N^2 + (1 + I_N)\left(1 - e^{-\theta x_N^2}\right) + \text{constant}$$

which implies

$$\frac{\partial\ ln(g_{DUSNR})}{\partial x_N} = \frac{1}{x_N} + 2\theta x_N\left[(1 + I_N)e^{-\theta x_N^2} - 1\right]$$

$$\frac{\partial^2 \ln(g_{DUSNR})}{\partial x_N^2} = -\frac{1}{x_N^2} - 4(1 + I_N)\theta^2 x_N^2 e^{-\theta x_N^2} - 2\theta\left[1 - (1 + I_N)\, e^{-\theta x_N^2}\right].$$

For $x_N > 0$, both $1/x_N^2$ and $e^{-\theta x_N^2}$ They are positive functions. If $x_N^2 > \ln(1 + I_N)\,/\theta$, then the second derivative becomes negative, indicating that the density function g_{DUSNR} Is log-concave. Since a log-concave density always has a unique mode, the theorem is thus proved.

3. Statistical properties

This section examines the basic mathematical characteristics of the "DUSNR distribution, such as the distribution of the rth order statistic, the moment-generating function, raw moments, the quantile function, and the Rényi entropy.

3.1. Moment generating function and raw moments

The expression for the moment generating function is given as $M_{X_N}(t) = E(e^{tX_N})$, where

$$E(e^{tX_N}) = \int_0^\infty e^{tx_N} \frac{2\theta(1+I_N)e^{1+I_N}}{e-1} x_N e^{-\theta x_N^2} e^{-(1+I_N)e^{-\theta x_N^2}} dx_N$$

$$= \frac{2\theta(1+I_N)}{e-1} e^{1+I_N} \int_0^\infty x_N\, e^{tx_N} e^{-\theta x_N^2} \sum_{m=0}^\infty \frac{(-1)^m}{m!} (1+I_N)^m e^{-m\theta x_N^2} dx_N$$

$$= \frac{2\theta e^{1+I_N}}{e-1} \sum_{m=0}^\infty \frac{(-1)^m}{m!} (1+I_N)^{m+1} \int_0^\infty x_N e^{-(m+1)\theta x_N^2 + tx_N} dx_N$$

$$= \frac{2\theta e^{1+I_N}}{e-1} \sum_{m=0}^\infty \frac{(-1)^m}{m!} (1+I_N)^{m+1} e^{t^2/4(m+1)\theta} \int_0^\infty x_N e^{-(m+1)\theta(x - t/2(m+1)\theta)^2} dx_N$$

$$= \frac{2\theta e^{1+I_N}}{e-1} \sum_{m=0}^\infty \frac{(-1)^m}{m!} (1+I_N)^{m+1} e^{t^2/4(m+1)\theta} \times$$

$$\left[\frac{e^{t^2/4(m+1)\theta}}{2(m+1)\theta} + \frac{t}{2(m+1)\theta} \int_0^\infty e^{-(m+1)\theta(x - t/2(m+1)\theta)^2} dx_N \right]$$

$$= \frac{e^{1+I_N}}{e-1} \sum_{m=0}^\infty \frac{(-1)^m}{m!} (1+I_N)^{m+1} e^{t^2/4(m+1)\theta} \frac{1}{(m+1)} \times$$

$$\left[e^{t^2/4(m+1)\theta} + t \int_0^\infty e^{-(m+1)\theta(x_N - t/2(m+1)\theta)^2} dx_N \right]$$

$$= \frac{e^{1+I_N}}{e-1} \sum_{m=0}^\infty \frac{(-1)^m}{(m+1)!} (1+I_N)^{m+1} \left[1 + te^{t^2/4(m+1)\theta} \int_0^\infty e^{-(m+1)\theta(x_N - t/2(m+1)\theta)^2} dx_N \right]$$

$$= \frac{e^{1+I_N}}{e-1} \sum_{m=0}^\infty \frac{(-1)^m}{(m+1)!} (1+I_N)^{m+1} \left[1 + \frac{\sqrt{\pi}\, t\, e^{t^2/4(m+1)\theta}}{2\sqrt{(m+1)\theta}} \operatorname{erfc}\left(\frac{-t}{2\sqrt{(m+1)\theta}} \right) \right]$$

Calculating the moments using the moment-generating function is tedious due to the complex form of the generating function. Therefore, we derive the raw moments by taking the direct expectations as follows: $E(X_N^r) = \int_0^\infty x_N^r \frac{2\theta(1+I_N)}{e-1} e^{(1+I_N)} x_N e^{-\theta x^2} e^{-(1+I_N)e^{-\theta x_N^2}} dx_N$

$$= \frac{2\theta e^{(1+I_N)}}{e-1} (1+I_N) \int_0^\infty x_N^{r+1} e^{-\theta x_N^2} \sum_{m=0}^\infty \frac{(-1)^m}{m!} (1+I)^m e^{-m\theta x_N^2} dx_N$$

$$= \frac{2\theta e^{(1+I_N)}}{e-1} \sum_{m=0}^\infty \frac{(-1)^m}{m!} (1+I_N)^{m+1} \int_0^\infty x_N^{r+1} e^{-(m+1)\theta x_N^2} dx_N$$

$$= \frac{\theta e^{(1+I_N)}}{e-1} \sum_{m=0}^\infty \frac{(-1)^m}{m!} (1+I_N)^{m+1} \frac{\Gamma(r/2+1)}{[(m+1)\theta]^{r/2+1}}$$

$$= \frac{e^{(1+I_N)}}{e-1} \frac{\Gamma(r/2+1)}{\theta^{r/2}} \sum_{m=0}^\infty \frac{(-1)^m}{m!} \frac{(1+I_N)^{m+1}}{(m+1)^{r/2+1}}.$$

The first two raw moments given below

$$E(X_N) = \frac{e^{(1+I_N)}}{e-1} \frac{\sqrt{\pi}}{2\sqrt{\theta}} \sum_{m=0}^\infty \frac{(-1)^m}{m!} \frac{(1+I_N)^{m+1}}{(m+1)^{3/2}},\ E(X_N^2) = \frac{e^{(1+I_N)}}{e-1} \frac{1}{\theta} \sum_{m=0}^\infty \frac{(-1)^m}{m!} \frac{(1+I_N)^{m+1}}{(m+1)^2}$$

are derived by imputing r = 1, 2. Consequently, the mean, variance and other higher-order moments can be found similarly.

3.2. Quantile function

The value of a random variable is defined using the quantile function in such a way that the chance that the variable will be less than or equal to that value is equal to the specified probability. For a DUSNR distribution with parameter θ, the distribution function of a random variable is such that $g_{DUSNR}\big(Q(p)\big) = p, p \in (0,1)$, which implies that

$$Q(p) = \sqrt{\frac{1}{\theta} ln\left(\frac{1+I_N}{1+I_N - ln\big((e-1)p+1\big)}\right)}.$$

To analyse the impact of the parameter on the shape of the distribution, the coefficients of skewness (B) and kurtosis (K) are computed using quantiles, which are defined as

$$B = \frac{Q(3/4) + Q(1/4) - Q(1/2)}{Q(3/4) - Q(1/4)}, \qquad K = \frac{Q(3/8) - Q(1/8) + Q(7/8) - Q(1/4)}{Q(3/4) - Q(1/4)}.$$

Also, the median of the DUSNR distribution is defined as Q(1/2).

3.3. Rényi Entropy

Rényi Entropy quantifies the uncertainty and diversity within a probability distribution, with higher values indicating greater unpredictability and lower values indicating more certainty. We calculate the entropy function of order w as

$$\tau_N(w) = \tfrac{1}{w-1} ln\big(\textstyle\int_0^\infty g_N^w(x_N)dx_N\big)$$

$$= \tfrac{1}{w-1} ln\left[\left(\tfrac{2\theta(1+I_N)}{e-1} e^{(1+I_N)}\right)^w \textstyle\int_0^\infty x_N^w e^{-w\theta x_N^2} e^{-w(1+I_N)e^{-\theta x_N^2}}\, dx_N \right]$$

$$= \frac{1}{w-1} ln\left[\left(\frac{2\theta(1+I_N)}{e-1} e^{(1+I_N)}\right)^w \sum_{m=0}^{\infty} \frac{(-1)^m}{m!} (1+I_N)^m \frac{w^m}{2} \frac{\Gamma((w+1)/2)}{\big((w+m)\theta\big)^{(w+1)/2}} \right]$$

$$= ln\big(2\sqrt{\theta}\big) + \frac{(1+I_N)w - ln(e-1)}{w-1} + \frac{1}{w-1} ln\left(\sum_{m=0}^{\infty} \frac{(-w)^m}{m!} (1+I_N)^{m+w} \frac{\Gamma((w+1)/2)}{(w+m)^{(w+1)/2}}\right).$$

3.3. Distribution of r^{th} ordered statistics

Order statistics are especially significant in reliability engineering and survival data analysis, where the hazard function is a key analytical tool. Suppose $(X_{N1}, X_{N2}, \dots, X_{Nn})$ Represent a neutrosophic sample of independent and identically distributed random variables holding a density. $g_N(x)$. If their ordered counterparts are denoted by $(X_{N(1)}, X_{N(2)}, \dots, X_{N(n)})$, then the PDF of the r^{th} order statistic $X_{N(r)}$ is

$$g_{(r)}(x_N) = \frac{n!}{(r-1)!\,(n-r)!} \left[\frac{e^{(1+I_N)\left(1-e^{-\theta x_N^2}\right)} - 1}{e-1}\right]^{r-1} \left[1 - \frac{e^{(1+I_N)\left(1-e^{-\theta x_N^2}\right)} - 1}{e-1}\right]^{n-r} \times$$

$$\frac{(1+I_N)\cdot 2\theta x_N e^{-\theta x_N^2}}{e-1}\cdot e^{(1+I_N)\left(1-e^{-\theta x_N^2}\right)}, \quad x_N>0.$$

The CDF of the r^{th} order statistic $X_{N(r)}$ is provided as

$$G_{(r)}(x_N)=\sum_{k=r}^{n}\binom{n}{k}\left[\frac{e^{(1+I_N)\left(1-e^{-\theta x_N^2}\right)}-1}{e-1}\right]^k\left[1-\frac{e^{(1+I_N)\left(1-e^{-\theta x_N^2}\right)}-1}{e-1}\right]^{n-k}, \quad x_N>0.$$

4. Parameter Estimation

The parameters are estimated based on sample observations drawn from the underlying distribution. In this study, data are generated from the DUSNR distribution with a parameter. θ, ensuring that the sample reflects the characteristics of the population under consideration. We adopt the following inverse transformation algorithm to generate random observations:

Algorithm 1:

1. Generate random observations $u_1, u_2, \dots, u_n$ from the U(0,1) distribution.
2. A random sample of size n, i.e., $x_{Ni}, i=1,2,\dots,n$ from DUSNR distribution is obtained from the equation $x_{Ni}=g_{DUSNR}^{-1}(u_i)$ which implies

$$x_{Ni}=\sqrt{\frac{1}{\theta}ln\left(\frac{1+I_N}{1+I_N-ln((e-1)u_i+1)}\right)}, i=1,2,\dots,n.$$

Using the random sample $\underline{x_N}=\{x_{N1},x_{N2},\dots.,x_{Nn}\}$ of size n, the likelihood function for the parameter θ from the DUSNR distribution is given by

$$L\left(\theta\middle|\underline{x_N}\right)=\prod_{i=1}^{n}g_{DUSNR}(x_{Ni},\theta)=\left(\frac{2\theta(1+I_N)}{e-1}\right)^n e^{n(1+I_N)}\prod_{i=1}^{n}\left(x_{Ni}e^{-\theta x_{Ni}^2}e^{-(1+I_N)e^{-\theta x_{Ni}^2}}\right).$$

The corresponding log-likelihood is calculated as

$$l=ln(L)=n\,ln(\theta)-\theta\sum_{i=1}^{n}x_{Ni}^2-(1+I_N)\sum_{i=1}^{n}e^{-\theta x_{Ni}^2}+\text{terms without }\theta.$$

To find the MLE for θWe calculated the first and second derivatives of the log-likelihood function with respect to θ. The following first derivative is used to find MLE.

$$\frac{\partial l}{\partial\theta}=\frac{n}{\theta}-\sum_{i=1}^{n}x_{Ni}^2+(1+I_N)\sum_{i=1}^{n}x_{Ni}^2e^{-\theta x_{Ni}^2}=0.$$

The likelihood equation can be solved to obtain the MLE using the *uniroot* function in R. This means that the log-likelihood function is concave since the second derivative is negative."

$$\frac{\partial^2 l}{\partial\theta^2}=-\frac{n}{\theta^2}-(1+I_N)\sum_{i=1}^{n}x_{Ni}^4e^{-\theta x_{Ni}^2}<0.$$

Hence, the MLE for θ Exists and is unique.

5. Simulation study

The efficiency of the MLE under the DUSNR distribution is analysed using the neutrosophic root mean square error. (RMSE_N). This measure quantifies the discrepancy between observed and estimated values, where a lower value. RMSE_N Signifies greater accuracy of the estimator. We define the expression for RMSE_N as

$$\mathrm{RMSE}_N = \sqrt{\frac{1}{m}\sum_{i=1}^{m}\left(\widehat{\theta_i} - \theta\right)^2}$$

Samples corresponding to I_N = 0, 0.5, (0.2, 0.7) are generated using Algorithm-1, and the simulation is replicated N = 10,000 times. The computations are performed in the R software. For each sample size n = 15, 50, 100, the RMSE_N Is evaluated. Table 1 presents the estimated bias and RMSE_N Associated with the MLE based on this simulation study.

Tabe 1:(Bias, RMSE_N) for MLE of θ

θ	I_N	n=15	n=50	n=100
0.2	0	0.0113, 0.0026	0.0029, 0.0006	0.0014, 0.0003
	0.5	0.3371, 0.1199	0.3276, 0.1089	0.3260, 0.1071
	(0.2,0.7)	(0.1514,0.4648), (0.0263,0.2250)	(0.1438,0.4537), (0.0215,0.2082)	(0.1426,0.4519), (0.0207,0.2054)
1	0	0.0282, 0.0163	0.0072, 0.0040	0.0036, 0.0020
	0.5	0.8427, 7495	0.8189, 0.6808	0.8149, 0.6619
	(0.2,0.7)	(0.3786, 1.1620), (0.1646, 1.4060)	(0.3596, 1.1344), (0.1348, 1.3014)	(0.3565, 1.1298), (0.1297, 1.2836)

The observations from the table:

1. Bias and MSE decrease as the sample size increases from n = 15 to n = 100 for all θ and I_N Values, indicating improved estimation accuracy with larger samples.

2. For I_N = 0 (no indeterminacy), the MLE performs well, with very small bias and MSE across all parameter settings.

3. When I_N = 1, both bias and MSE are notably higher than in the case of I_N = 0, showing that neutrosophic uncertainty degrades estimation precision.

6. **Applications**

This section applies the proposed model to COVID-19 mean incubation time data, emphasising the importance of accurately modelling incubation periods for effective disease control and forecasting. The data given in Table 2 have been used previously by Cheng et al. (2021).

Table 2: Mean Incubation Periods with Uncertainties for COVID-19

(7.82, 8.37)	(8.24, 9.88)	(4.95, 5.40)	(7.55, 8.88)	(4.15, 5.89)	(6.87, 7.04)
(5.43, 6.52)	(4.79, 5.89)	(6.87, 7.55)	(5.52, 6.73)	(5.08, 6.93)	(6.62, 7.45)
(3.33, 4.67)	(4.90, 5.57)	(6.61, 7.10)	(3.92, 5.09)	(8.18, 9.24)	(6.62, 7.11)
(5.48, 6.62)	(4.18, 5.97)	(5.50, 7.18)	(9.96, 11.09)	(8.04, 9.44)	(7.37, 8.99)
(5.28, 6.65)	(9.99, 10.70)	(10.66, 11.68)	(8.27, 9.09)	(5.12, 5.78)	(5.43, 6.19)
(4.84, 6.16)	(4.38, 5.40)	(6.45, 7.39)	(6.33, 7.79)	(5.58, 6.02)	(2.21, 3.47)
(7.39, 8.25)	(6.21, 6.86)	(6.01, 7.31)	(6.30, 7.43)	(5.61, 6.64)	(5.82, 6.49)
(5.26, 5.81)	(2.21, 3.23)	(7.51, 8.01)	(4.34, 5.13)	(4.67, 5.23)	(4.31, 4.96)

Incubation time varies across diseases and is crucial for estimating exposure and planning treatment strategies. Due to challenges in measuring exact exposure times, available data often include uncertainties. Given the presence of uncertainty in the data, the conventional Rayleigh and neutrosophic Rayleigh models are extended through the proposed DUSNR distribution, which enables interval-based inference for the parameter.

The study assesses the effectiveness of the DUSNR distribution as a modelling framework, with the AIC and BIC values in Table 3 indicating a superior fit compared to both the standard Rayleigh and neutrosophic Rayleigh models. The MLEs under each model are also provided in Table 3, demonstrating their practical utility in analysing real-world epidemiological datasets.

Table 3: Parameter estimation and assessment of distribution fit

Model	MLE	AIC	BIC
Rayleigh	(0.01923, 0.0253)	(53.896, 81.48)	(55.767, 83.35)
Neutrosophic Rayleigh	(0.01923, 0.0253)	(11.801, 39.40)	(13.68, 41.27)
DUSNR	(0.0284, 0.0372)	(6.06, 32.64)	(7.74, 33.42)

7. Conclusion

This study introduced the DUSNR distribution, a unique expansion of the Rayleigh family that can efficiently describe data under uncertainty, imprecision, and indeterminacy. By combining the DUS transformation and the neutrosophic framework, the suggested model improves the capacity of classical distributions to handle real-world data that is frequently ambiguous or incomplete. Quantiles, moments, the moment-generating function, and order statistics have all been properly derived. Simulation studies were used to test model parameter estimation processes, and the results showed that as the sample size increased, estimator performance improved. Furthermore, the application to an actual dataset confirmed the DUSNR distribution's practical utility, with AIC and

BIC values indicating that it fits better than existing Rayleigh-based models. Overall, the DUSNR model provides a strong statistical tool for assessing imprecise or uncertain data, opening up new avenues for research in neutrosophic statistics and its applications.

Funding: This research received no external funding.

Acknowledgements: The authors sincerely appreciate the editorial team for their valuable guidance and support during the review process.

Conflicts of Interest: The authors declare no conflict of interest.

References

1. Ahsan-ul-Haq, M. (2022). Neutrosophic Kumaraswamy Distribution with Engineering Application. *Neutrosophic Sets and Systems*, *49*, 269–276.
2. Algamal, Z. Y., Alobaidi, N. N., Hamad, A. A., Alanaz, M. M., and Mustafa, M. Y. (2024). Neutrosophic Beta-Lindley Distribution: Mathematical Properties and Modelling Bladder Cancer Data. *International Journal of Neutrosophic Science*, *23*(2), 186–194.
3. Alhabib, R., Ranna, M. M., Farah, H., and Salama, A. A. (2018). Some Neutrosophic Probability Distributions. *Neutrosophic Sets and Systems*, *22*, 30–38.
4. Alhasan, K. F. H., and Smarandache, F. (2019). Neutrosophic Weibull Distribution and Neutrosophic Family Weibull Distribution. *Neutrosophic Sets and Systems*, *28*(1), 191–199.
5. Aslam, M. (2024). The Neutrosophic Negative Binomial Distribution: Algorithms and Practical Application. *REVSTAT-Statistical Journal*.
6. Atanassov, K. T. (1999). Intuitionistic Fuzzy Sets. *Studies in Fuzziness and Soft Computing, Physica-Verlag, Heidelberg, Germany*, *35*, 1–37.
7. Banerjee, P., and Bhunia, S. (2022). Exponential transformed inverse Rayleigh distribution: Statistical properties and different methods of estimation. *Austrian Journal of Statistics*, *51*(4), 60–75.
8. Belohlavek, R., Dauben, J. W., and Klir, G. J. (2017). *Fuzzy logic and mathematics: a historical perspective.* Oxford University Press.
9. Cheng, C., Zhang, D., Dang, D., Geng, J., Zhu, P., Yuan, M., Liang, R., Yang, H., Jin, Y., & Xie, J. (2021). The incubation period of COVID-19: A global meta-analysis of 53 studies and a Chinese observation study of 11,545 patients. *Infectious Diseases of Poverty*, *10*(1), 119.
10. Hassan, M. K., and Aslam, M. (2024). Birnbaum–Saunders distribution for imprecise data: statistical properties, estimation methods, and real-life applications. *Scientific Reports*, *14*.
11. Jamal, F., Shafiq, S., Aslam, M., Khan, S., Hussain, Z., and Abbas, Q. (2024). Modelling COVID-19 data with a novel neutrosophic Burr-III distribution. *Scientific Reports*, *14*.
12. Khan, M. I., and Mustafa, A. (2023). Powered inverse Rayleigh distribution using DUS transformation. *International Journal of Analysis and Applications*, *21*, 61–61.
13. Khan, Z., Amin A., Khan S. A., and Gulistan M. (2022). *Statistical Development of the Neutrosophic Lognormal Model with Application to Environmental Data. Neutrosophic Sets and Systems, 47*, 1–11.

14. Khan, Z., Gulistan, M., Kausar, N. and Park, C. (2021). Neutrosophic Rayleigh Model with Some Basic Characteristics and Engineering Applications. *IEEE Access*, *9*, 1–10.
15. Khan, Z., and Al-Bossly, A. (2021). On Statistical Development of Neutrosophic Gamma Distribution with Applications to Complex Data Analysis. *Mathematical Problems in Engineering*.
16. Norouzirad, M., Rao, G. S., and Mazarei, D. (2023). Neutrosophic Generalised Rayleigh Distribution with Application. *Neutrosophic Sets and Systems, 58*(1), 250–262.
17. Patro, S. K., and Smarandache, F. (2016). The Neutrosophic Statistical Distribution: More Problems, More Solutions. *Neutrosophic Sets and Systems, 12*, 73–79.
18. Rao, G. S. (2023). Neutrosophic Log-Logistic Distribution Model in Complex Alloy Metal Melting Point Applications. *International Journal of Computational Intelligence Systems, 16*(1), 1–12.
19. Sherwani, R. A. K., Naeem, M., Aslam, M., Raza, M. A., Abid, M., and Abbas, S. (2021). Neutrosophic Beta Distribution with Properties and Applications. *Neutrosophic Sets and Systems, 41*, 209–214.
20. Tripathi, H., and Agiwal, V. (2024). A new version of the univariate Rayleigh distribution: properties, estimation and its application. International Journal of System Assurance Engineering and Management. *International Journal of System Assurance Engineering and Management, 15*(11), 5367–5377.
21. Vladutescu, S., Colhon, M. (2020). *New Challenges in Neutrosophic Theory and Applications*.
22. Zeina, M. B., and Hatip A. (2021). Neutrosophic random variables. *Neutrosophic Sets and Systems, 39*, 44–52.

Received: Aug 15, 2025. Accepted: Feb 22, 2026